Tilt Effects on GWR Superconducting Gravimeters

U. Riccardi, J. Hinderer, J.-P. Boy, y. Rogister

To cite this version:

U. Riccardi, J. Hinderer, J.-P. Boy, y. Rogister. Tilt Effects on GWR Superconducting Gravimeters. Journal of Geodynamics, Elsevier, 2009, 48 (3-5), pp.316. 10.1016/j.jog.2009.09.001 . hal-00594423

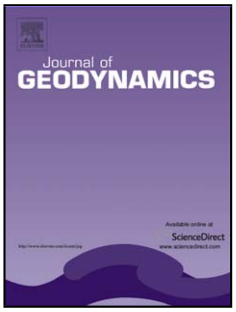

Title: Tilt Effects on GWR Superconducting Gravimeters

Authors: U. Riccardi, J. Hinderer, J.-P. Boy, Y. Rogister

PII: S0264-3707(09)00068-4
DOI: doi:10.1016/j.jog.2009.09.001
Reference: GEOD 895

To appear in: *Journal of Geodynamics*

Please cite this article as: Riccardi, U., Hinderer, J., Boy, J.-P., Rogister, Y., Tilt Effects on GWR Superconducting Gravimeters, *Journal of Geodynamics* (2008), doi:10.1016/j.jog.2009.09.001

Tilt Effects on GWR Superconducting Gravimeters

Riccardi U. [1, 2], **Hinderer J.**[2], **Boy J.-P.** [2,3], **Rogister Y.** [2]

[1] Dipartimento di Scienze della Terra, Università "Federico II" di Napoli, L.go S. Marcellino 10, 80138 Naples, Italy. Fax:+390815527631; +33690240291

[2] Institut de Physique du Globe de Strasbourg- (UMR 7516 CNRS-Université de Strasbourg), 5 rue René Descartes, 67084 Strasbourg Cedex, France.
[3] Planetary Geodynamics Laboratory, Mail Code 698, NASA Goddard Space Flight Center, Greenbelt, MD 20771, USA.

ABSTRACT

The superconducting gravimeters (SGs) are the most sensitive and stable gravity sensors currently available. The low drift and high sensitivity of these instruments allow to investigate several geophysical phenomena inducing small and long-period gravity changes. In order to study such topics, any kind of disturbance of instrumental origin has to be identified and possibly modelled. A critical point in gravity measurement is the alignment of the gravimeter to the local vertical. In fact a tilt of the instrument will lead to an apparent gravity change and can affect the instrumental drift. To avoid these drawbacks, SGs are provided with an "Active Tilt Feedback System" (ATFS) designed to keep the meter aligned to the vertical. We analyze tilt and environmental parameters collected near Strasbourg, France, since 1997 to study the source of the tilt changes and check the capability of the ATFS to compensate them. We also present the outcomes of a calibration test applied to the ATFS output to convert the Tilt Power signals into angles. We find that most of the observed signal has a thermal origin dominated by a strong annual component of about 200 μrad. Nevertheless, our analysis shows that even the tilt due to different geophysical phenomena, other than the thermal ones, can be detected. A clear tidal signal of about 0.05 μrad is detectable thanks to the large data stacking (> 11 years). We conclude that (i) the ATFS device compensates the tilt having a thermal origin or coming from any sources and (ii) no significant tilt changes alter the gravity signal, except for the high-frequency (> 1 mHz) perturbations.

Keywords: Superconducting gravimeter, Tilt output Calibration, Gravity

Corresponding author: Riccardi U.; e-mail: umberto.riccardi@unina.it

1. Introduction

The superconducting gravimeters (SGs) are the most sensitive and stable gravity sensors currently available for ground-based measurements. The inherent stability of the SGs enables them to detect signals from a sampling time of 1 s up to several years with a time-domain accuracy of 1nm/s^2 = 0.1 μGal or better (Richter et al., 1995; Rosat et al., 2004) and down to 0.5 nm/s^2 in the frequency domain (Rosat et al., 2004). The SG is a device that uses magnetic levitation of a superconducting sphere instead of a mechanical spring as in the case of a classical gravimeter. The sensitivity of SG approaches one nGal (10^{-11} ms^{-2}), which corresponds to 10^{-12} of the surface gravity, and drift rates are as low as a few μGal per year. These features allow us to study many geophysical phenomena inducing gravity changes over a broad time-scale range, such as seismic free oscillations, earth tides, ocean and atmospheric loads, post-glacial rebound, seasonal water storage variations and so on (Hinderer & Crossley, 2000; 2004). In order to match such topics, any kind of disturbance of instrumental origin has to be modelled and subtracted from the raw gravity signal. It is of central importance in gravity measurement to align the gravimeter to the local vertical. In fact a tilt of the instrument will lead to an apparent gravity change and can affect the instrumental drift. This effect could deteriorate the quality of the collected data and hide real gravity changes. In principle, all of the aforementioned geophysical sources induce elasto-gravitational deformation of the Earth, and, therefore, a tilt of the ground (e.g. Rerolle et al., 2006; Jahr et al., 2006). Also the daily and seasonal temperature variations produce thermal waves which propagate into the ground and produce the well known thermo-elastic deformation (Berger, 1975). Besides these natural sources, the ambient conditions in the laboratory have to be taken into account. For instance temperature-related tilt signals may be caused by the periodic turning on and off of the air conditioning system. Moreover, air drafts on the dewar can produce rapid variations in horizontal pressure, while temperature changes cause unequal thermal expansion of the dewar walls. Either will produce tilt by causing the top of the dewar to move slightly. In order to avoid all these effects, SGs are provided with an “Active Tilt Feedback System” (ATFS) designed to keep the meter aligned to the vertical to better than a few μradians (GWR Instruments Inc., 1985).

If a gravimeter is tilted by an angle ϕ, from the local vertical, it measures the component of gravity $g \cos\phi$, along its axis. For ϕ is small, the difference between the gravity g and the projection $g \cos\phi$ of g onto the gravimeter axis is $g\phi^2/2$, to the second order in ϕ. Of course, the apparent gravity $g \cos\phi$, which is measured by the gravimeter, is smaller than g. The apparent decrease in the gravity is about -4.9 x 10^{-3} nm s^{-2} μrad^{-2}. However, for the SGs, there is an apparent increase in the measured gravity. The tilt sensitivity of the SG is opposite to that of the ideal gravimeter because of the geometry of the magnetic field that levitates the sphere. When the SG is tilted, the horizontal component of gravity pushes the sphere away from the axis of the coil. Since the vertical force due to the magnetic field decreases radially from the axis, the sphere falls down as the instrument deviates from the vertical, resulting in an apparent increase in gravity. Thus the gravimeter outputs a minimum value of gravity when it is properly levelled (GWR Instruments Inc., 1985).When the meter is properly levelled, we reach what is called the “Tilt Insensitive Position” (TIP). It is a very important parameter because it measures the extent to which instrumental tilts will induce spurious gravity signals. To reduce this effect, it is recommended that the levelling of the SG be annually checked (Warburton, 1998).

The ATFS consists of: 1) tiltmeters, 2) tilt electronics, 3) thermal levellers (TLs), 4) support frame. Tilt variation of the gravimeter is detected by two tiltmeters, which are orthogonally positioned just above gravity sensing unit at 4K and corresponding analog voltages are sent to the tilt control electronics (GEP-2). Users can record these signals (X, Y “Tilt Balance”). In an active feedback operation, the balance signals generate feedback currents (Left, Right “Tilt Power”) for the TLs. Heat expansion elements inside the TLs expand or shrink according to supplied power and keep the Tilt Balance signals nulled to zero. The TLs mechanically tilt the gravimeter through the support frame. They are designed to control only long- period tilt signals - down to about 15 minutes. This implies that the influence of tilt on the seismic band is not accounted for. Higher frequency tilt signals, as those related to earthquakes, are not compensated and they will appear on both the X and Y Tilt Balance signals and gravity. The TLs also have a manual height adjustment element; the gravimeter is tilted by rotating the micrometer head on top of the TL assembly. This device is used for coarse levelling and fine adjustment of the TIP.

There are two types of ATFS-geometries used in SGs: one model is suspended from the top by the support frame while the other is mounted on the base (Iwano & Fukuda, 2004). Both types have the same mechanism in which the support frame has three legs, one is fixed and the others are controlled by the TLs. The two axes of the support frame are linked to two tiltmeters. For the top-mounted type (old ones with a big dewar) the support frame is a right isosceles triangle and its orthogonal axes are aligned with the tiltmeter axes. For the bottom-mounted type (“SG C type”, having a Compact dewar and most recent “OSG” meters), the support frame is an equilateral triangle and the directions of the support frame and tiltmeters axes are not aligned. The SG C-026 at the J9 station in Strasbourg is of the bottom-mounted type; the geometry and orientation of its tilt frame are illustrated in Fig. 1. The advantage of the isosceles support frames (top-mounted type) is that the left and right axes are orthogonal and the two tiltmeters can be aligned with these axes. For the sake of the usual procedure of levelling of the gravimeter this means, in the SETUP mode, that a change of the X (or Y) micrometer does not affect the null position measured by the other micrometer.

In order to study the tilt changes at J9, we analyzed more than eleven years of Tilt Power and environmental parameters, namely temperature and humidity, collected since 1997. We evaluate the capability of the ATFS to compensate the tilt changes preserving the verticality of the meter and detect and study the “sources” of the observed tilt changes.

As the scale factors for the SGs ATFS are not provided by the manufacturing company (GWR Instruments Inc.), we face the problem of the TLs output calibration. Here we present a calibration test applied to the Tilt Power signal from the ATFS and its validation by using different methodological approaches.

2. Data analysis and results

The J9 gravity station hosts the superconducting gravimeter C026 (SG-C026) in a bunker 15 km from Strasbourg, where it has been operating since July 1996. The meter has a compact dewar (volume: 125 l) and a tilt frame sizing 28 inches (711.2 mm). It is the bottom mounted type; the geometry and orientation of its tilt frame are illustrated in Fig. 1. The meter is located in a separate gravity room that is somewhat thermally separated from the rest of the equipment, including the devices for the room temperature control and the helium compressor. To decouple mechanically the SG from the building it operates on a concrete pillar that is isolated from the floor and connected to the bedrock. This should minimize the disturbances transmitted from environmental noise or human activity in the building. . In November 1999 an air dryer device was installed to control the room temperature and humidity; it has a switching cycle on/off triggered by a set humidity value and uses fans to distribute the air. The meter is shielded with a styrofoam panel to avoid direct air drafts on the dewar. The SG-C026 is routinely calibrated, 6 times per year on the average, by means of parallel recording with the absolute gravimeter FG5 #206 (Amalvict et al., 2001; Amalvict & Hinderer, 2007). A maintenance experiment, aimed at checking the tilt compensation system, was performed in 2007 by the GWR Instruments Inc. staff. It was developed in two phases: a) gravimeter levelling by means of micrometer changes; b) fine adjustment of the levelling through electronic reset changes. The data allowed us to check the stability of the TIP coordinates;they were slightly different from the values measured when the gravimeter was installed in 1996. Indeed, during more than 11 years the tilt has changed by about 6.5 mils (equivalent height change = 0.16

mm), which represents about 225 μrad for the J9 support frame; assuming a linear time change, a rate of about 20 μrad/year is obtained. A similar offset from the true vertical was found by Van Camp and Francis (2007) at Membach (Belgium) station after 10 years of operation. Accounting for the typical accuracy (0.3 mils) for the TIP setting, we can conclude that only small changes affected the SG verticality in more than 11 years.

This experiment was only performed twice to avoid instrumental disturbances.

To study the tilt changes at J9, a 4116-days long (more than 11 years) data-set has been analysed (Fig. 2). The collected signals are the “Tilt Power” outputs from Left and Right TLs (Figs. 2a and 2b) and environmental data (temperature and humidity of the SG room) (Figs. 2c and 2d) from 1997 February 22nd to 2008 June 3rd. A strong negative correlation between Tilt Power and temperature is quite evident (Fig. 2). The TLs are activated by heat, so it is expected that the tilt control voltages will correlate very well with the room temperature.

Fig. 2d clearly displays that the ambient conditions at the J9 gravity station sharply changed after the setup of the air dryer device at the end of 1999; the mean humidity in the room falls down from 75% to 40%. The drawback of this installation is that the air dryer has “coloured” the ambient noise with a characteristic spectral signature due to the cycling switching on/off triggered by a temperature sensor. The spectral signature consists in a main peak at the frequency 24 *cycles/day* (cpd) [period = 1hour] and higher harmonics (48 cpd, 72 cpd, 96 cpd). These spectral features appeared since the time of the air dryer setup; almost all of the geophysical instruments installed in J9 are affected by this background noise. Moreover the room temperature (Fig. 2c) has been strongly influenced by a massive tree cutting above and around the building in February 1999 to install a permanent GPS antenna. As a consequence, the seasonal variation of the room temperature increases from 4°C to 6°C peak-to-peak. This is likely because the shadowing of the woody cover has disappeared. Since 2007 a further remarkable step-like increase (about 2.4°C peak-to-peak) in the room temperature has to be pointed out; this is imputable to the increase of the heating sources coming from new equipments (data acquisition system for SG and a weather station).

2.1. Calibration of the Thermal Levellers output

Because the scale factors for the ATFS are not provided by the manufacturing company, we apply a calibration procedure to the TLs to convert the tilt voltages into angles. We perform the calibration of the TLs’ output voltages by inducing variations in the height of the free legs of the support frame through a known micrometer turn; the units of the micrometer dial are “mils”. The conversion factor furnished by GWR is that 4 complete dial revolutions (= 100 mils) correspond to a height change of 2.54 mm. Knowing the length of the support frame, we convert the micrometer mils into angles. The calibration test is done by setting the tilt electronics GEP-2 in the RUN mode to activate feedback on any tilt changes. When the tilt levelling system is operating in tilt feedback, the ATFS responds to the frame tilting by adjusting the power to the TLs to keep the tiltmeter reading (Tilt Balance) at a null voltage. Starting with the left micrometer we perform the calibration by inducing several step-like changes in the TL height through precise dial turning and operating on the micrometers one by one. To avoid possible sources of systematic errors and remove any backlash out of the micrometer, we first overshot the targeted dial value, then turn down to it. The elapsed time between two steps is about 30 minutes so that the disturbance fades out. The TLs output during the calibration test is shown in Fig. 3. After the signal is stabilized, we fit the data to the micrometer changes, the latter being converted into angle units. A least-square fit (Figs. 3b, 3d) provides the scale factors to convert TL voltages into angles (Tab. 1).

We setup a validation test to check the calibration obtained by means of the micrometer manipulations. The spectral features of the available data-set allow us to use a different methodological approach to calibrate the Tilt Power signal. The amplitude spectra of the hourly decimated Tilt Power and room temperature are drawn in Fig. 4; only the long-term polynomial trend is removed from the signals. The spectra clearly show the existence in both the temperature and Tilt Power signals of an annual harmonic component (frequency = 0.00273 cpd) (Figs. 4a, 4c) and peaks in the solar bands at 1 cpd, 2 cpd and harmonics (Figs. 4a, 4b). Zooming in on the frequency range 0 – 4 cpd (Fig. 4b), we see that the temperature spectrum displays a single peak at 2cpd, as expected, and the spectra of the Tilt Power are characterized by a double peak: the first one at the thermal frequency of 2 cpd and the second one at a frequency of 1.93 cpd, in the range of the M2 tidal band. To separate the spectral components having a thermal origin from the tidal ones, a coherence analysis has been performed (Fig. 5). Actually we use an approach slightly different from the classic cross-spectral analysis in defining coherence function . We computed a set of frequency–dependent cross-correlation factors. The procedure, described by Riccardi et al. (2007), can be summed up as follows: first, we filter the time-series by means of a set of pass-band filters with a narrow bandwidth (0.01 cpd), then we apply a regression analysis to the filtered signals and account for the correlation factors in each frequency band. Considering that the “coherence function” is a cross-correlation in the frequency domain, our procedure is equivalent to the classic one. The main advantage of this approach is that it provides the sign of the coherence to investigate whether there is an inverse or direct correlation in each frequency band, summing up the information coming from both the amplitude and phase cross-spectrum. We apply this analysis to, first, the Tilt Power and temperature, and, next, the Tilt Power and theoretical tilt due to the solid Earth tide. As expected, the correlation between TL and temperature signals is characterized by two features: (i) a background level scattering around a mean value - 0.5 and (ii) a line spectrum at the harmonics of the day (1 cpd, 2 cpd) owing to the effect of the solar heating; there is no line at the M2 frequency. On the contrary, the coherence between the TL and body tide shows a background scattering around 0 and a line spectrum at the harmonics (0.93 cpd, 1 cpd, 1.93 cpd, 2 cpd), which include high-amplitude tidal waves O1, PSK1, and M2. So, we conclude that the spectral peak at 1.93 cpd has a tidal origin. It is noteworthy that the sensitivity of the ATFS is good enough to detect the tilt associated to the solid Earth tides, provided that the time-series of the Tilt Power are sufficiently long to allow a suitable stacking of the "weak" tidal signal.

Consequently, we use the theoretical tides to calibrate the TL outputs. We compute the tilt due to both the body tides, for the Wahr-Dehant (WD) Earth model, (Dehant et al., 1999) and the ocean tide loading (OTL) (Boy et al., 2003) according to model FES04 (Letellier, 2004; Lyard et al., 2006). We obtain the scale factors from the ratio between the spectral amplitudes of the theoretical tidal signal and Tilt Power: the results are listed in Tab. I. As the OTL effect is only available for North-South and East-West directions, we applied this correction exclusively to the Right TL, which is almost East-West oriented (ref. Fig. 1). The results obtained in the frequency domain match pretty well those collected by the micrometer manipulations; they deviate less than 10% from each other.

Still willing to validate the calibration factors, we make a tidal analysis (Wenzel, 1996) of the Tilt Power signals calibrated by using the factors coming from the calibration test. For the M2 tidal wave, we obtain a tidal tilt factor (γ) and a phase in agreement with the Earth models (Tab. II) (Wenzel, 1996; d'Oreye, 2003; Jahr et al., 2006).

2.2. Analyses of the calibrated Tilt Power signal

In order to get insight into the possible sources of the observed tilt changes, we filter out the different components (Fig. 6) of the signal to make a better correlation analysis between the Tilt Power and temperature in different spectral bands. In fact, the Tilt Power and temperature time series show common features at different frequencies: a polynomial long-term trend and an annual periodic signal. The detrended and low-pass filtered (*cut-off frequency = 0.01 cpd*) time series are plotted in Figs. (6a), (6b) and (6c). By subtracting them from the raw signals, we obtain the high-frequency components shown in Figs (6d), (6e) and (6f). We apply the frequency dependent correlation analysis to the filtered data to investigate the linearity of the temperature influence on the Tilt Power signal and recover the thermal admittance function (Fig. 7). To better define the transfer function of the temperature effect on Tilt Power, we compute a frequency dependent admittance. Both the correlation function and admittance have the smallest negative values at low frequency (< 0.5 cpd) and at the frequency of the thermal harmonics (1 cpd, 2 cpd...). This implies that the Tilt Power and temperature are almost perfectly anti-correlated and that most of the TL signal has a thermal origin. The good coherence at low frequencies comes from the annual variation of both the temperature and Tilt Power, which dominates the signals. The behaviour of the admittance function in the frequency domain confirms these results (Fig. 7); in fact, the thermal influence on Tilt Power in the different spectral bands closely follows the correlation function.

Finally, we tried to address the question whether uncompensated tilts can affect the observed gravity changes. We compute the gravity variation due to the observed tilt changes (Fig. 8a) accounting for the previously mentioned tilt dependence of 4.9×10^{-3} nm/s^2/μradian^2.

In case the SG should operate without the ATFS, which keep the meter vertical, tilt changes would induce a huge gravity signal; it would be as large as the solid Earth tides, making the meter unusable for gravity record. Moreover we check whether only the non-thermal tilt was uncompensated by the ATFS. To separate the thermal and non-thermal Tilt Power signals, we use the frequency dependent admittance coefficients as parameters for the transfer function of the temperature influence on the Tilt Power. The Tilt Power signal reduced for the thermal effect is drawn in the Fig. (8b) and (8c). The high amplitudes of the residual signal from 1997 till 2000 show that the transfer function of the thermal effect computed by means of the admittance coefficients is inefficient in the first part of the time series; this is probably because we have neglected the time variation of the amplitude of the thermal effects. The temperature variations in the room were actually larger before the installation of the device for the temperature control in November 1999. That was also the case in 2002, when the air dryer was switched off during about two months to study the noise it generates.

Fig. (8d) displays the gravity variation induced by the non-thermal tilt changes. Just for having a comparison between a well known gravity signal and the gravity effect due to the non-thermal tilt changes, we also plot the gravity variation associated to the polar motion. This enables us to have an idea of the amount of the gravity signal that could be induced if the observed tilt was uncompensated. To answer definitely the question whether any inefficiency of the ATFS could alter the gravity signal, we compare the residual gravity changes (Fig. 8e) and the equivalent gravity effect due to the non-thermal tilt changes; they look uncorrelated. This means there is no obvious significant gravity variation due to uncompensated tilt.

3. Conclusions

To quantify the tilt sensed by superconducting gravimeter C-026, located 10 km north of Strasbourg, France, we have calibrated the Thermal Levellers (TLs) of the Active Tilt Feedback System (ATFS). As the TLs are activated by heat, the Tilt Power signals have mainly a thermal origin so it's not supposed to be real tilt. However our analysis shows that the tilt due to different geophysical phenomena, other than the thermal ones, can affect the collected Tilt Power signals. Actually a clear tidal signal sticks out from the time series; anyway it is hard to separate in the Tilt Power signal the real tilt from the pure thermal effect. Three simultaneous sources actually contribute to the recorded Tilt Power signals. The biggest one is the direct reaction of the TL to the room temperature changes; in that case the TLs behave as thermometers, but with a characteristic phase lag as long as 20 min. Furthermore feedback currents are generated by the tiltmeters in response to the tilt of the SG, which could be due to geophysical phenomena, e.g. the body tides; hydrology, ground deformation and to the thermo-elastic deformation due to the propagation of thermal waves into the building and surrounding ground. In fact the thermal expansion and contraction in response to daily and seasonal temperature fluctuations generate real movements of the building and pillar hosting the SG that are detected by the tiltmeters and other sensors. Even if the room temperature did not vary, real tilts up to several microradians would occur because of the daily heating and cooling of the pillar and building.

As expected we find that most of the observed Tilt Power signal has a thermal origin.

In summary, we detect:

(i) a long-term trend of about 20 µrad/year,
(ii) a strong annual component of about 200 µrad peak-to-peak,
(iii) a diurnal component having an amplitude of 0.3 µrad,
(iv) a semi-diurnal component of about 0.1µrad (the harmonics S3 and S4 are also evident),
(v) a clear tidal component as large as 0.05 µrad in the semi-diurnal band.

The tidal effects clearly appear thanks to the large data stacking (> 11 years); moreover they provide us with a tool to validate the results of the TLs calibration made by means of the micrometer height changes. It is noteworthy that Tilt Power signals contain not only the temperature changes, but even low amplitude tidal tilt signals. The tidal signals are likely detected by the tiltmeters inside the gravity sensing unit and routed to the TLs as feedback currents. Anyway it is hard to separate one signal from the other, namely recognizing which device senses the tilt changes. A step ahead would consist in installing an independent tilt sensor, for instance a bi-axial tiltmeter, aligned with the internal SG tiltmeters. This would enable us to better discriminate between the thermal signal and the real tilt.

Thus we can conclude the efficiency of the ATFS device is at a suitable level to guarantee high accuracy gravity measurements and inherent time stability. TLs are very sensitive to the room temperature, but any changes in temperature or coming from whatever sources are correctly balanced, except for the high-frequency perturbations (period < 15 min) so that no significant tilt changes alter the gravity signal. It follows that it is not recommended to let the meter operate without this tilt compensation system, because the tilt changes would remarkably affect the measured local gravity as a whole and the long-term trend signal (drift) too.

Acknowledgements The authors thank W. Zürn and T. Jahr for their valuable comments that significantly improved the paper.

References

Amalvict, M., Hinderer, J., Boy, J.-P., Gegout, P., 2001. A 3 years comparison between a superconducting gravimeter (GWR C026) and an absolute gravimeter (FG5-206) in Strasbourg (France). J. Geodetic Soc. Japan 47 (1), 334–340.

Amalvict, M. and J. Hinderer, 2007. Is the calibration factor stable in time? paper presented at First Asian Workshop on SGs, Taiwan, March 2007.

Berger J., 1975. A Note on Thermoelastic Strain and Tilts. Journ. Geoph. Res., vol 80, pp 274-277.

Boy, J.-P., Llubes, M., Hinderer, J. and Florsch, N., 2003. A comparison of tidal ocean loading models using superconducting gravimeter data, J. Geophys. Res., 108, 2193, doi: 10.1029/ 2002JB002050.

Dehant, V., Defraigne, P., Wahr, J.M., 1999. Tides for a convective Earth. Journal of Geophysical Research 104 (B1), 1035–1058.

d'Oreye de Lantremange N., 2003. Inclinomètre à niveaux hydrostatiques de haute résolution en géophysique. Thèse présentée en vue de l'obtention du titre de Docteur en Sciences, Université Catholique de Louvain, 340 pp.

GWRInstruments Inc., 1985. Superconducting Gravity Meter Model TT70 Cryogenic Refrigeration Operating Manual. San Diego, 179 pp.

Hinderer, J. and D. Crossley 2000. Time Variations and Inferences on the Earth's Structure and Dynamics, Surveys in Geophysics, 21, 1-45.

Hinderer, J. and D. Crossley 2004. Scientific achievements from the first phase (1997–2003) of the Global Geodynamics Project using a worldwide network of superconducting gravimeters, Journal of Geodynamics, 38, 237-262.

Iwano S., Fukuda Y 2004. Superconducting gravimeter observations without a tilt compensation system. Physics of the Earth and Planetary Interiors, 147: 343–351, doi: 10.1016/j.pepi.2004.08.001.

Jahr T., Letz H., Jentzsch G., 2006. Monitoring fluid induced deformation of the earth's crust: A large scale experiment at the KTB location/Germany. Journal of Geodynamics 41, 190–197.

Letellier, T., 2004. Etude des ondes de marée sur les plateux continentaux. Thèse doctorale, Université de Toulouse III, Ecole Doctorale des Sciences de l'Univers, de l'Environnement et de l'Espace, 237pp.

Lyard F., Lefévre F., Letellier T., Francis O., 2006. Modelling the global ocean tides: Modern insights from FES2004. Ocean Dynam 56(5–6): 394–415.

Rerolle T., Florsch N., Llubes M., Boudin F., Longuevergne L. 2006. L'inclinométrie, un nouvel outil pour le suivi temporel des aquifères? C. R. Geoscience 338 : 775–786.

Riccardi U., Hinderer J., Boy J., 2007. On the Efficiency of Barometric Arrays to Improve the Corrections of Atmospheric Effects on Gravity Data. Physics of the Earth and Planetary Interiors, 161, 224-242.

Richter, B., Wenzel, H.G., Zurn, W., Klopping, F., 1995. From Chandler wobble to free oscillations: comparison of cryogenic and other instruments in a wide period range. Phys. Earth Planet. Int. 91, 131–148.

Rosat, S., Hinderer, J., Crossley, D., Boy J-P., 2004. Performance of superconducting gravimeters from long-period seismology to tides. Journal of Geodynamics, 38, 461–476.

Van Camp M., Francis O., 2007. Is the instrumental drift of superconducting gravimeters a linear or exponential function of time? J. Geod. 81:337–344, DOI 10.1007/s00190-006-0110-4.

Warburton R. J., 1998. Optimizing the performance of the SG during the GGP. Presentation at 1st GGP Workshop July 1997 (Bruxelles), online: http://www.eas.slu.edu/GGP/gwrwrk1.html.

Wenzel, H.-G., 1996. The nanogal software: Earth tide data processing package ETERNA 3.30. Bulletin d'Information des Marèes Terrestres 124, 9425–9439.

Table and Figure Captions

Table I: Results of the TLs' output calibration through micrometer changes and its validation in the frequency domain. The values of the ratio between the spectral amplitudes of the theoretical tidal signal and Tilt Power are listed in the last two columns; the last ones have been computed for an ocean-less Earth (WD = Wahr-Dehant Earth model) and also accounting for the OTL effect (FES04).

Table II: Parameters (γ and phase) for M2 tidal wave determined by means of harmonic analyses on Tilt Power signals; in the last two lines the theoretical values are given as a reference.

Figure 1: Geometry and orientation of the tilt support frame and internal tiltmeters for the SG-C026 meter operating in Strasbourg gravity station J9.

Figure 2: The Strasbourg hourly data sets from February 1997 until June 2008: (a) Left Tilt Power; (b) Right Tilt Power; (c) room temperature; (d) room humidity. A polynomial fitting is plotted to emphasize the existence of a long-term parabolic trend in both the Tilt Power and temperature signals.

Figure 3: Output signals collected during the calibration test and fit results: (a, c) Left and Right Tilt Power outputs; (b, d) results of the least square fit; the values in the inset represent the micrometer changes expressed in mils.

Figure 4: Amplitude spectrum of the Tilt Power signals and room temperature (a); detail focused on the tidal bands (b); detail focused on the lowest frequencies (c) to emphasize the annual peak.

Figure 5: Correlation coefficients coming from a frequency-dependent regression analysis of the Left TL output versus both theoretical tilt tide and temperature.

Figure 6: De-trended and filtered Tilt Power and temperature: (a)-(c) signals de-trended by means of a polynomial fitting (grey curve) and low-pass filtered ones (black curve); (d)-(f) high-pass filtered signals.

Figure 7: Correlation coefficients resulting from a frequency-dependent regression between Tilt Power signals and temperature; the thermal admittance is plotted too.

Figure 8: Modelling of the equivalent gravity effect due to the tilt changes: (a) gravity effect due to the tilt changes (black curve); the solid Earth tide is plotted for the sake of comparison (grey curve). (b, c) Residual Left and Right Tilt Power signals reduced for thermal effect; (d) equivalent gravity effect induced by tilt signal plotted in (b) and (c); The gravity changes due to the Polar Motion (grey curve) is also drawn to have a reference; (e) Residual gravity computed for J9 station.

Table I

	Micrometer changes			**Spectral Ratio**	
TLs	**mils/V**	**mm/V**	**μrad/V**	**WD** (μrad/V)	**WD**+FES04 (μrad/V)
Left	16.8 ± 0.2	0.427 ± 0.003	200 ± 2	182	Undetermined
Right	15.05 ± 0.08	0.382 ± 0.002	179 ± 1	162	170 ± 11

Table II

	γ	**Phase (°)**
Right_TL	0.84 ± 0.09	1.48 ± 6.0
Left_TL	0.77 ± 0.06	-174.3 ± 4.5
WD	0.70	0
WD+FES04	0.81	2.1

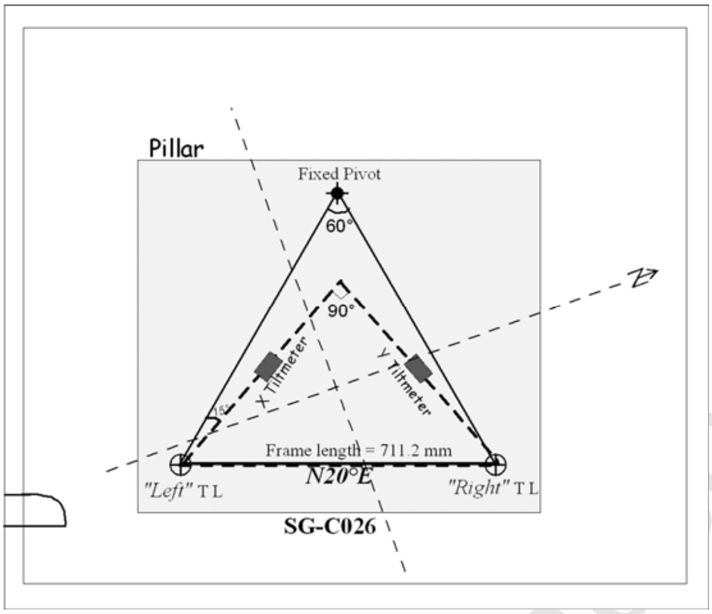
Pillar
Fixed Pivot
60°
N
90°
X Tiltmeter
Y Tiltmeter
15°
Frame length = 711.2 mm
N20°E
"Left" T L
"Right" T L
SG-C026

Figure 1

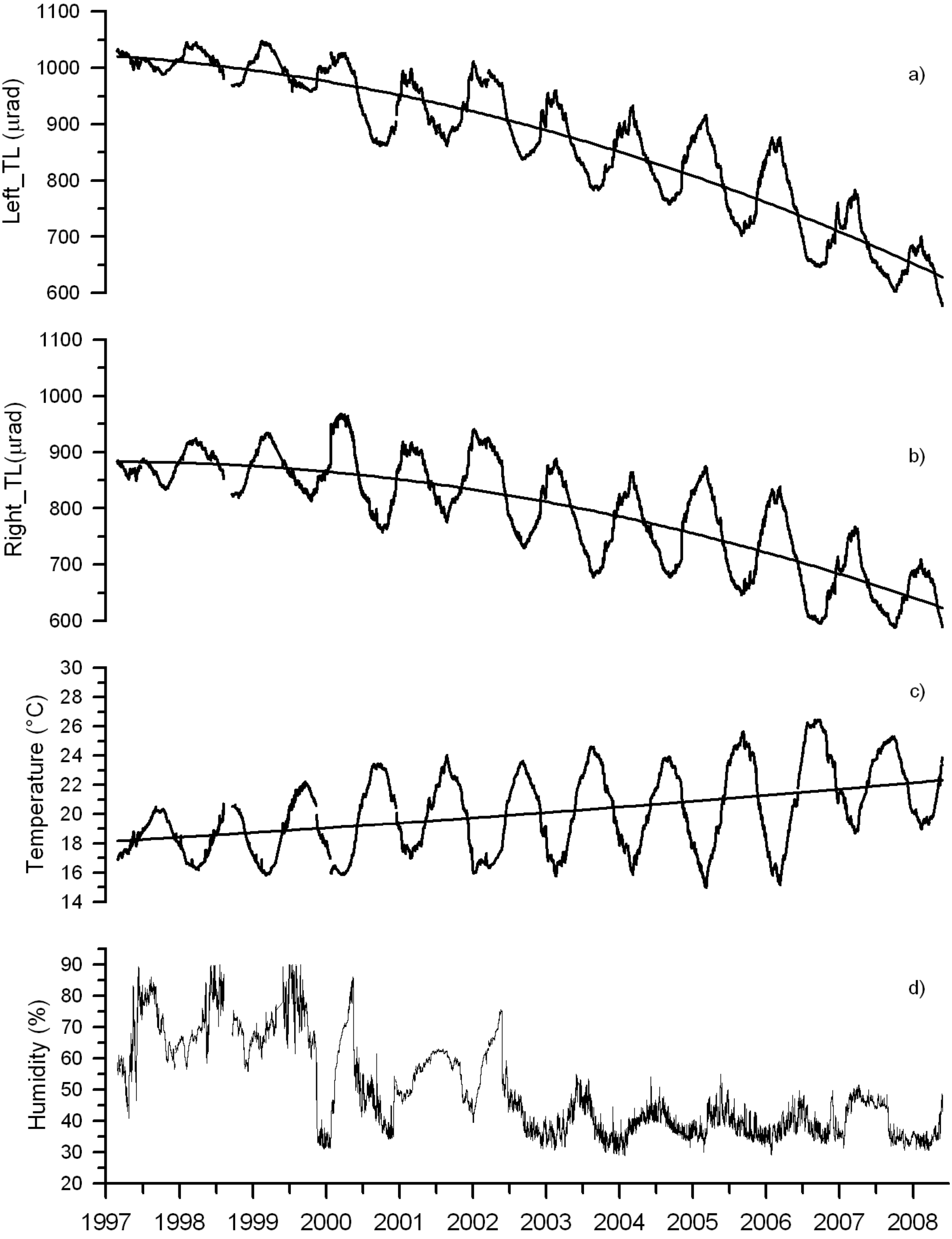
1100
1000
900
800
700
600
Left_TL (μrad)
a)
1100
1000
900
800
700
600
Right_TL(μrad)
b)
30
28
26
24
22
20
18
16
14
Temperature (°C)
c)
90
80
70
60
50
40
30
20
Humidity (%)
d)
1997
1998
1999
2000
2001
2002
2003
2004
2005
2006
2007
2008

Figure 2

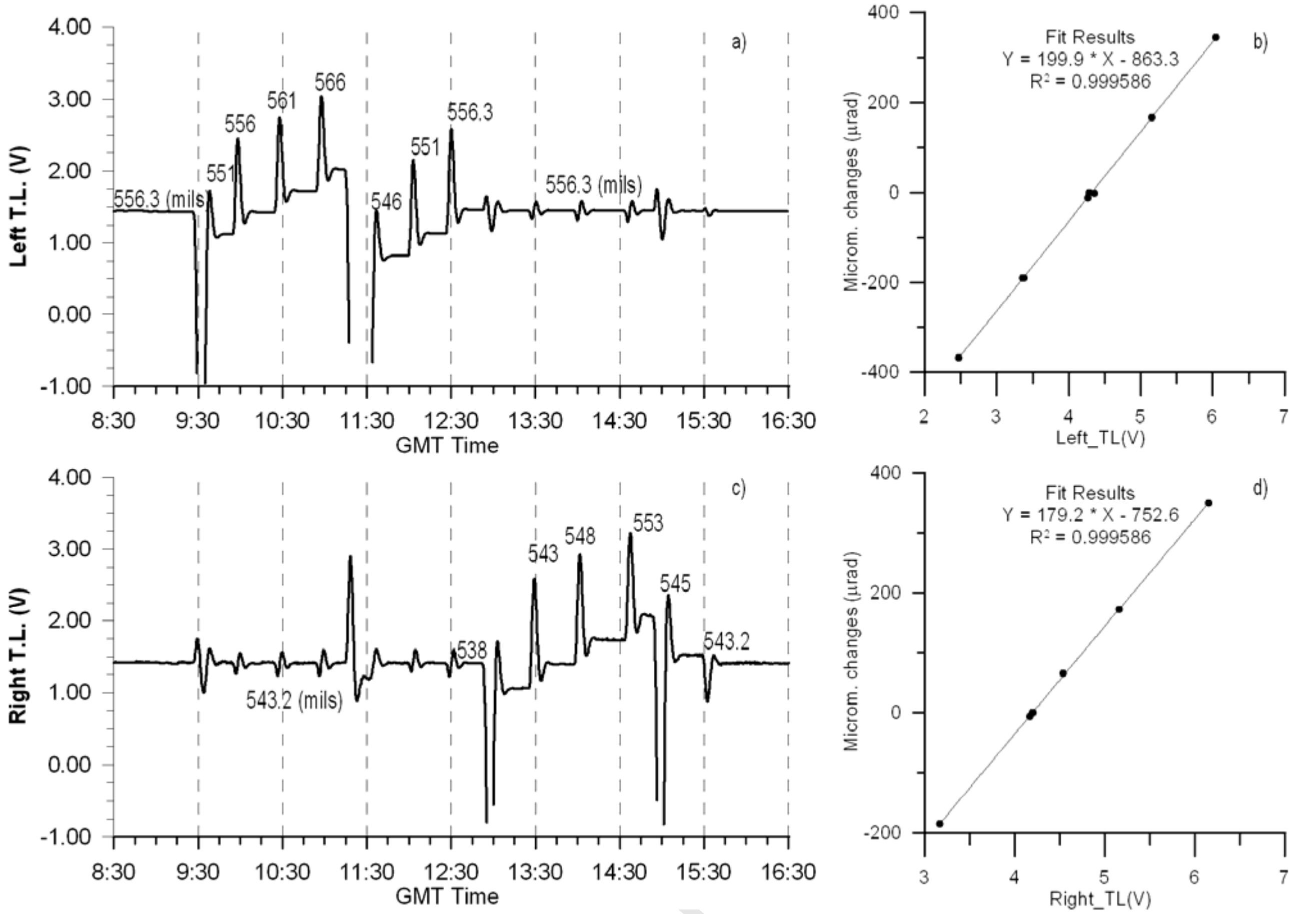
a)
Left T.L. (V)
4.00
3.00
2.00
1.00
0.00
-1.00
556.3 (mils)
551
556
561
566
546
551
556.3
556.3 (mils)
8:30
9:30
10:30
11:30
12:30
13:30
14:30
15:30
16:30
GMT Time
b)
Fit Results
Y = 199.9 * X - 863.3
R² = 0.999586
Microm. changes (µrad)
400
200
0
-200
-400
2
3
4
5
6
7
Left_TL(V)
c)
Right T.L. (V)
4.00
3.00
2.00
1.00
0.00
-1.00
543.2 (mils)
538
543
548
553
545
543.2
8:30
9:30
10:30
11:30
12:30
13:30
14:30
15:30
16:30
GMT Time
d)
Fit Results
Y = 179.2 * X - 752.6
R² = 0.999586
Microm. changes (µrad)
400
200
0
-200
3
4
5
6
7
Right_TL(V)

Figure 3

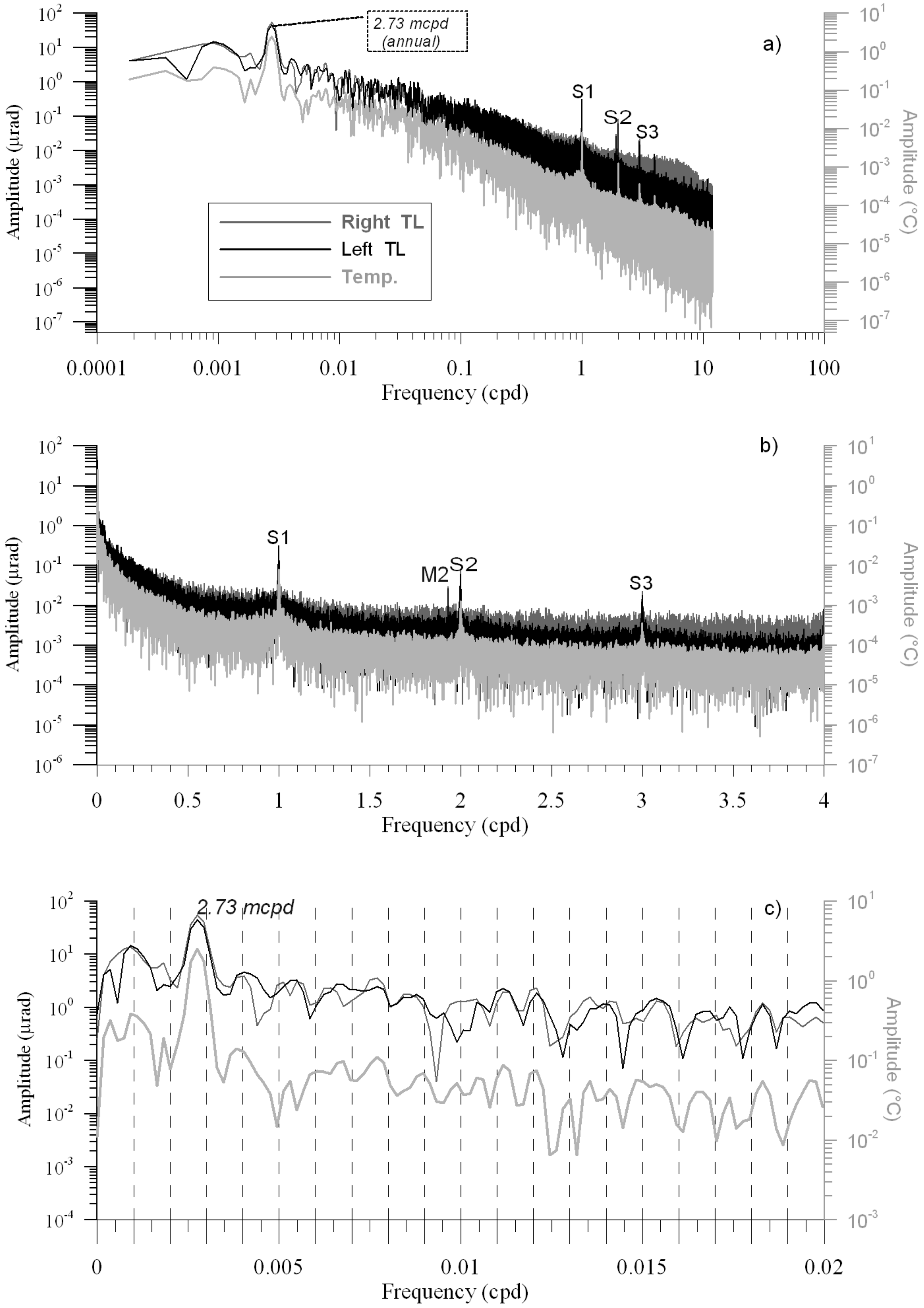
a)
2.73 mcpd
(annual)
S1
S2
S3
Right TL
Left TL
Temp.
Amplitude (µrad)
Amplitude (°C)
Frequency (cpd)
0.0001
0.001
0.01
0.1
1
10
100
b)
S1
M2
S2
S3
0
0.5
1
1.5
2
2.5
3
3.5
4
c)
2.73 mcpd
0
0.005
0.01
0.015
0.02

Figure 4

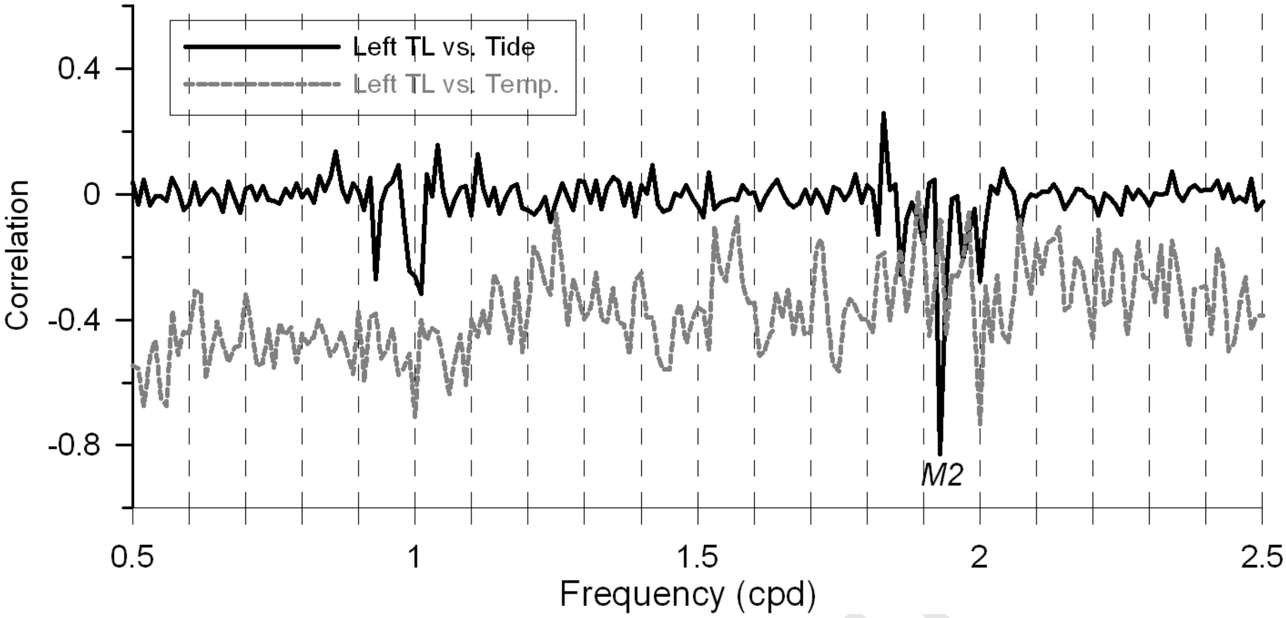
Left TL vs. Tide
Left TL vs. Temp.
Correlation
0.4
0
-0.4
-0.8
M2
0.5
1
1.5
2
2.5
Frequency (cpd)

Figure 5

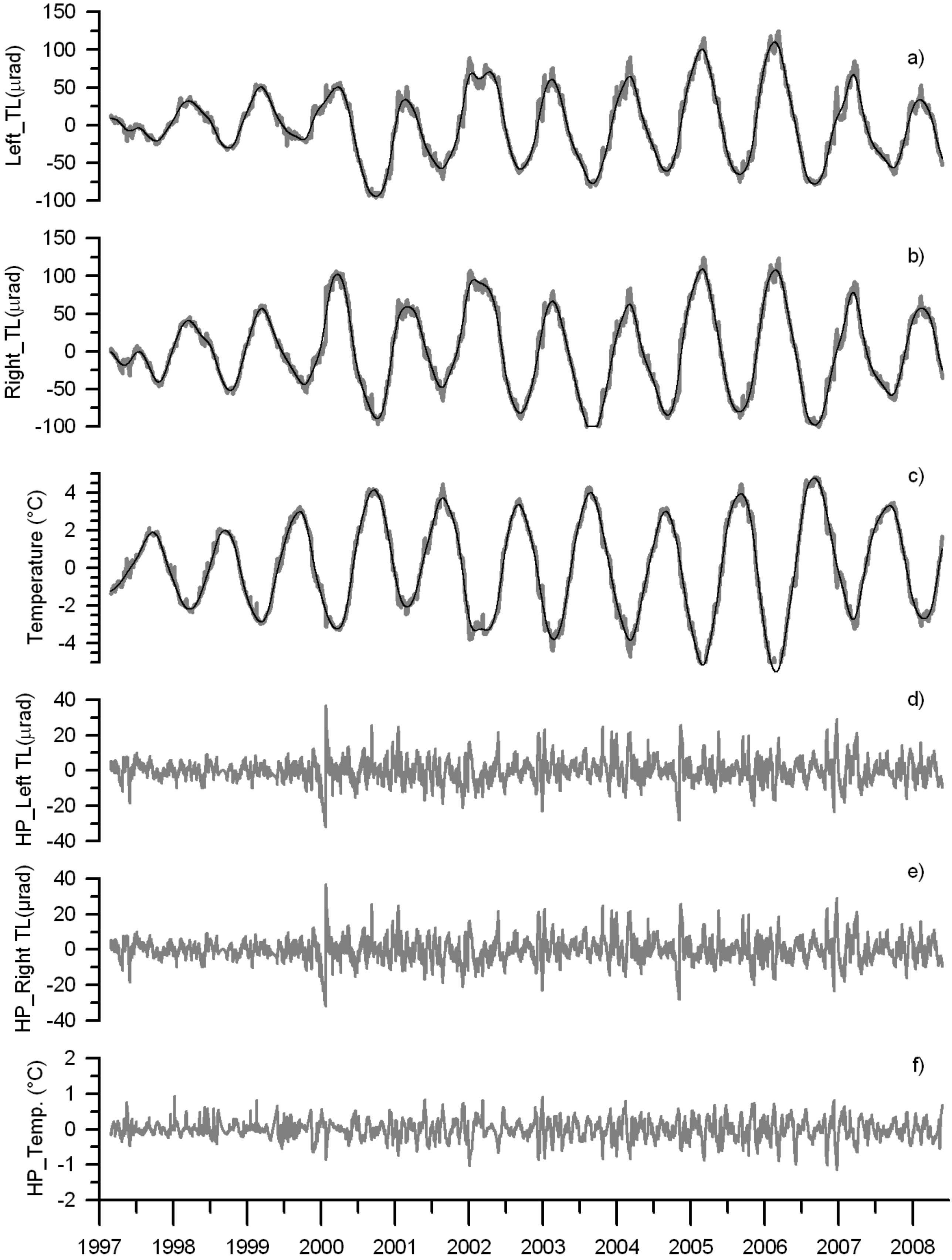
a)
b)
c)
d)
e)
f)
Left_TL(μrad)
Right_TL(μrad)
Temperature (°C)
HP_Left TL(μrad)
HP_Right TL(μrad)
HP_Temp. (°C)
150
100
50
0
-50
-100
4
2
0
-2
-4
40
20
0
-20
-40
2
1
0
-1
-2
1997
1998
1999
2000
2001
2002
2003
2004
2005
2006
2007
2008

Figure 6

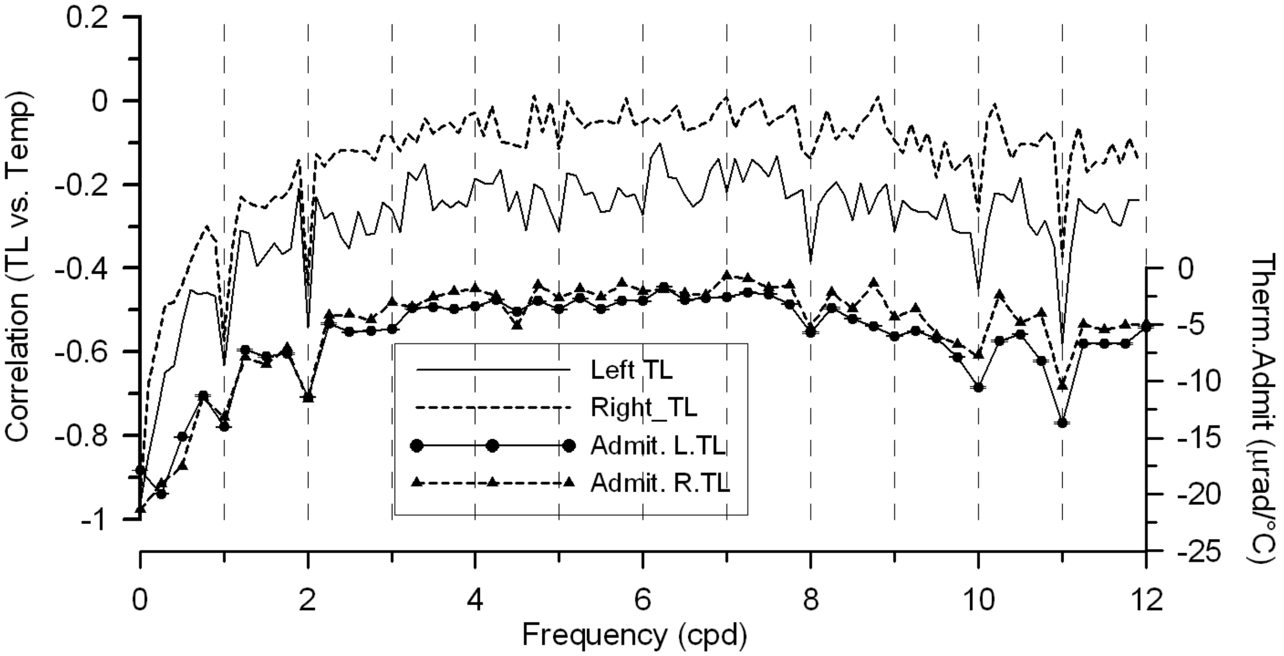
0.2
0
-0.2
-0.4
-0.6
-0.8
-1
Correlation (TL vs. Temp)
0
-5
-10
-15
-20
-25
Therm.Admit (µrad/°C)
0
2
4
6
8
10
12
Frequency (cpd)
Left TL
Right_TL
Admit. L.TL
Admit. R.TL

Figure 7

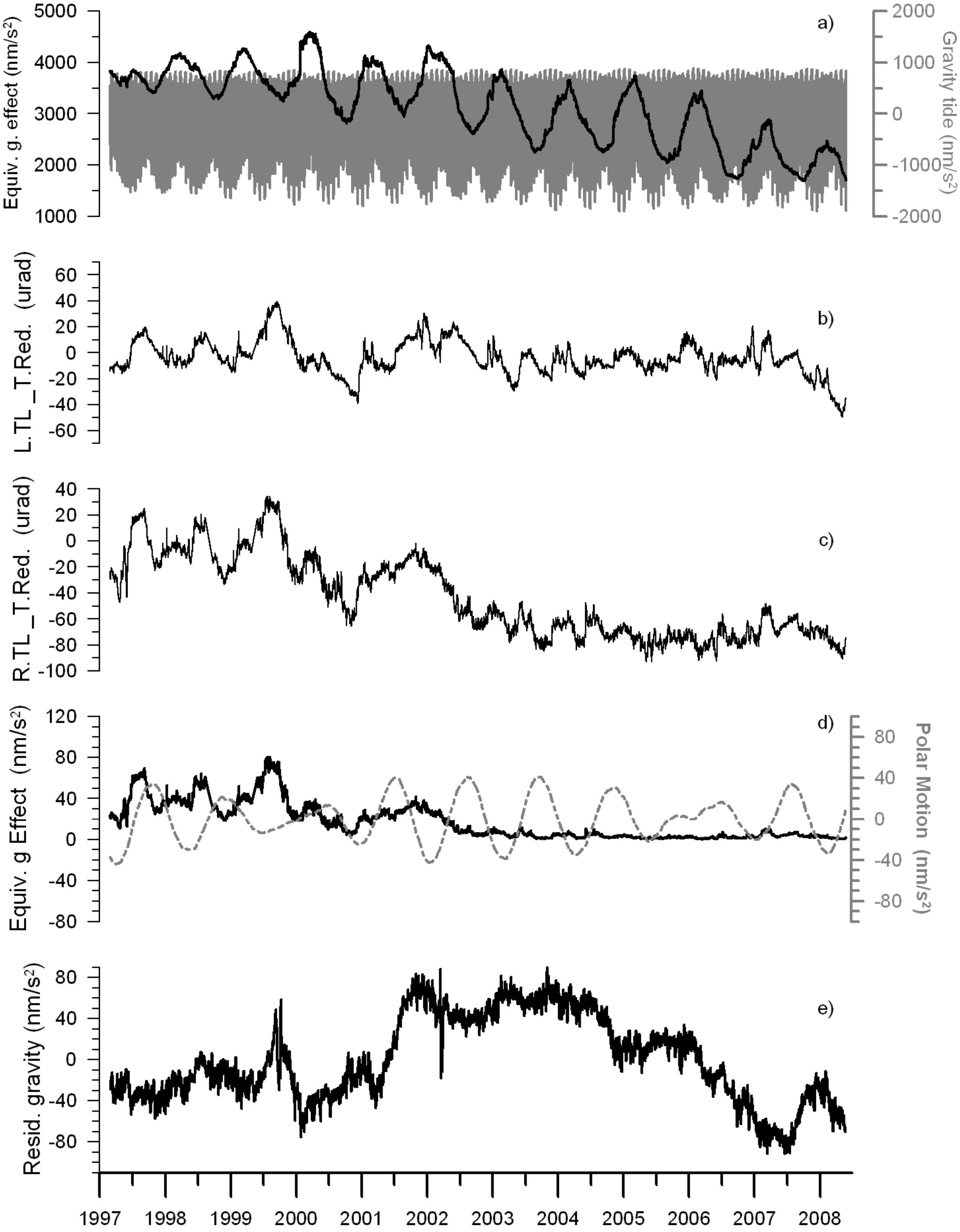
a)
Equiv. g. effect (nm/s^2)
5000
4000
3000
2000
1000
Gravity tide (nm/s^2)
2000
1000
0
-1000
-2000
b)
L.TL _T.Red. (urad)
60
40
20
0
-20
-40
-60
c)
R.TL _T.Red. (urad)
40
20
0
-20
-40
-60
-80
-100
d)
Equiv. g Effect (nm/s^2)
120
80
40
0
-40
-80
Polar Motion (nm/s^2)
80
40
0
-40
-80
e)
Resid. gravity (nm/s^2)
80
40
0
-40
-80
1997
1998
1999
2000
2001
2002
2003
2004
2005
2006
2007
2008

Figure 8